Cold Regions Science and Technology, 20 (1991) 11-23
Elsevier Science Publishers B.V., Amsterdam

Wave-induced iceberg motion

J.H. Lever[a,1], K. Klein[b], D. Mitchell[b] and D. Diemand[a,2]
[a] *U.S. Army Cold Regions Research and Engineering Laboratory (CRREL), 72 Lyme Road, Hanover, New Hampshire, USA*
[b] *Centre for Cold Oceans Resources Engineering (C-CORE), Memorial University of Newfoundland (MUN), St. John's, Newfoundland, Canada*

(Received July 6, 1990; accepted after revision December 5, 1990)

ABSTRACT

Lever, J.H., Klein, K., Mitchell, D. and Diemand, D., 1991. Wave-induced iceberg motion. *Cold Reg. Sci. Technol.*, 20: 11-23.

This paper describes the results of a three-year field study to measure the wave-induced motion of icebergs. We sought this information to examine how well iceberg velocities, derived using wave-tank tests, reflect those of irregularly shaped full-scale icebergs. We deployed self-contained motion-monitoring packages on icebergs in the Labrador Sea and on the Grand Banks, and obtained 19 data sets of wave-induced iceberg motion. To our knowledge, these are the only available data describing the wave-induced motion of full-scale icebergs in six degrees-of-freedom.

For comparison with laboratory results, we computed normalized significant surge and heave iceberg velocities and plotted these against normalized peak wavelength. This demonstrated that velocities based on wave-tank study of four regularly shaped model icebergs do reflect the range of variation in iceberg motion attributable to random shape. The paper concludes that iceberg significant velocities are random quantities for a given size iceberg in a given sea state, and that a gamma probability density, fitted to wave-tank results, is suitable for describing their variations.

Introduction

To build an oil production platform able to survive on the Grand Banks of Newfoundland, engineers must consider the possibility of iceberg impact. Depending on the site, they may employ either a fixed or floating platform configuration and an overall philosophy of iceberg resistance or iceberg avoidance. They must then determine the iceberg impact design loads for the platform. To optimize the design, they must trade-off ice-strengthening costs, down-time costs associated with iceberg avoidance, and the consequences of impacts sufficient to damage the platform. The studies of Andersson et al. (1986), Salvalaggio and Rojansky (1986), Fuglem et al. (1989), and Holthe (1989), among others, illustrate various ways to incorporate iceberg-impact analyses into platform design. All such design analyses require, in some form, knowledge of iceberg population, size, shape, strength and velocity statistics, plus estimates of iceberg-management efficiencies.

To estimate iceberg-impact velocity statistics, researchers have used both physical and numerical models to describe how icebergs respond in a given sea state (see, for example, Andersson et al., 1986; Isaacson, 1987; Lever et al., 1987, 1989; Pawlowski and Wishahy, 1987). By necessity, all these models make simplifying assumptions about the forces involved (physical models neglect scale distortion of viscous forces, numerical models use potential flow with simple drag-coefficients to account for fluid viscosity). Most models incorporate the randomiz-

[1]Formerly with Faculty of Engineering and Applied Science, MUN.
[2]Formerly with C-CORE.

ing effects of irregular seas using linear superposition. Also, all analyses to date model iceberg geometry using regular shapes (cubical, spherical, cylindrical, etc.) despite the observational evidence indicating icebergs are in fact quite randomly shaped.

To address some of these concerns, Lever et al. (1988a) conducted a wave-tank study of four regular iceberg shapes (cubical, cylindrical, trapezoidal, spherical). Results from the three cubical models showed that, at least over a limited model-scale range (70:1 to 210:1), Reynolds number distortion did not significantly influence the measured motions. They also found that linear superposition quite accurately described iceberg motion characteristics in irregular seas. However, they did find that model shape had a strong influence on measured motions. Subsequent study (Lever et al., 1988b) confirmed that these shape differences do influence iceberg wave-induced velocity statistics. A key question thus remains: How well do velocity statistics derived for regular shapes reflect those of randomly shaped full-scale icebergs?

The objective of the present work was to obtain field measurements of wave-induced iceberg motion as a function of iceberg size and sea state. With these measurements, we hoped to assess the validity of physical and numerical modeling of this phenomenon. We conducted a pilot study in the Labrador Sea in 1984 to confirm that we could successfully deploy and recover self-contained, iceberg motion-monitoring packages. We then deployed upgraded packages on icebergs in the Labrador Sea in 1985 and on the Grand Banks in 1986 and 1987. Out of a total of 23 such deployments, we obtained 19 usable data sets of wave-induced iceberg motion. To our knowledge, these are the only available data describing the wave-induced motion of full-scale icebergs in six degrees-of-freedom. This paper describes the instrumentation and field techniques developed, and it presents the data in comparison with corresponding model predictions.

Instrumentation

We constructed two identical six degree-of-freedom iceberg motion-monitoring packages for this study. These packages were entirely self-contained and required no on-ice time for personnel during either deployment or recovery. They were extremely rugged, waterproof, deployable by either helicopter or vessel, and recoverable from the iceberg or out of the water. An earlier paper (Lever et al., 1986) describes these packages in some detail; we will only summarize their key features here.

Each package contained the following motion sensors: three servo-accelerometers, with ± 1 g dynamic ranges, to measure linear acceleration along orthogonal axes; a vertical gyro to measure pitch and roll (angular rotations about orthogonal axes) with ranges of $\pm 60°$ for pitch and $360°$ for roll; a flux-gate compass to measure magnetic bearing. The six sensor signals passed through individual low-pass filters (no attenuation below about 2 Hz, then increasing attenuation to -40 dB at 6 Hz). A multiplexer, operating at 12 Hz, combined these six signals and two reference voltages for storage on a single channel of an instrumentation recorder. This arrangement provided a minimum recording capacity of 1.5 h per deployment, adequately meeting our requirements.

For deployment of each package, we mounted the sensor cluster, power supply and filter boards, and instrumentation recorder on an aluminum plate; we then installed these within box-type enclosures constructed of 0.6 cm aluminum plate. The bottom half of each enclosure contained three 12 VDC batteries to provide power. We used O-rings to seal the enclosure halves and fitted the bottoms with four 5-cm-long tapered stainless steel pins to hold the packages on the iceberg. Figure 1 shows a schematic of the motion-monitoring packages. Once sealed, each package measured 0.66 m$\times$0.66 m$\times$0.51 m high, exclusive of the mating flange and tapered pins. The total mass of each package was about 100 kg, a value insignificant compared with iceberg masses.

We calibrated the packages under both static (constant tilt) and dynamic conditions (circular motion of 1 m radius, adjustable frequency). When fully processed, the measured accelerations, velocities and displacements agreed with the imposed values to within about $\pm 5\%$ over the wave-period range of interest, 5–15 s. We felt this accuracy was sufficient for our purposes.

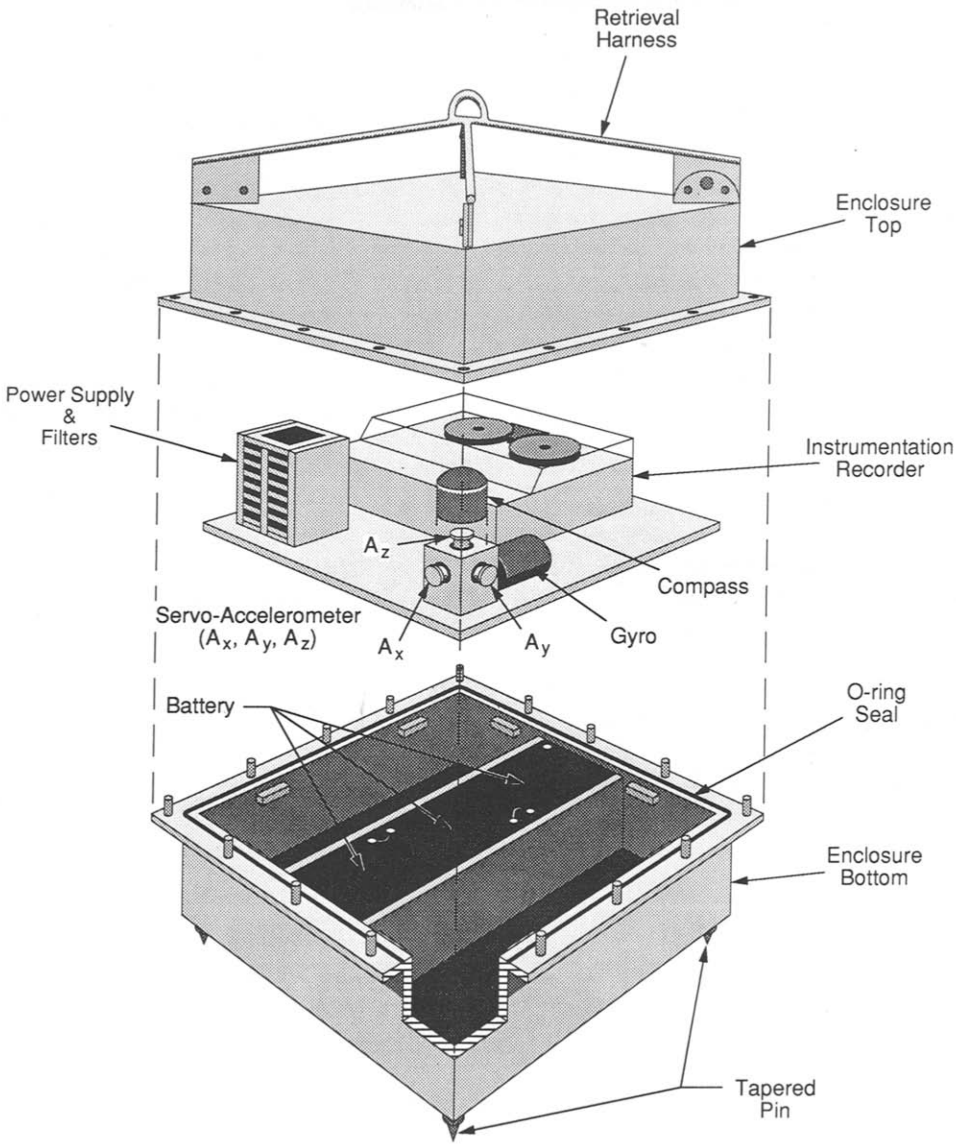

Fig. 1. Schematic of motion-monitoring packages showing principal elements.

Data acquisition

Labrador Sea deployments

During August, 1985, we conducted fifteen deployments of the two motion-monitoring packages off Cape Makkovik in the Labrador Sea. We ran this program in cooperation with the Dynamics of Iceberg Grounding and Scouring (DIGS) experiment (see Hodgson et al., 1988). We deployed the packages using a twin-engine helicopter, and recovered them either off the iceberg by helicopter or out of the water from a small vessel stationed nearby for this purpose.

To determine the sea state during each package deployment, we obtained the data from a wave buoy, moored nearby as part of the DIGS experiment. These data took the form of nondirectional, wave-energy period spectra, and they covered all but three deployment intervals. All package deployments occurred within 50 km of this moored buoy.

We also attempted to deploy a drifting wave buoy from the vessel stationed next to the iceberg of interest. While we succeeded in doing this for the first few package deployments, it became too difficult to track the drifting buoy and recover the motion-monitoring package in the event of the iceberg rolling. However, this buoy did provide significant wave-height and peak-period estimates for the deployment intervals not covered by the moored buoy.

To document the size and shape of each iceberg studied, we took numerous surface and aerial photographs, the former generally from at least the four principal compass headings. The known dimensions of the package enclosures provided us with means to scale these photographs and hence obtain the dimensions of the icebergs. From the measured maximum waterline length, L, waterline width, W, and maximum height, h (all in metres), we later estimated the mass, M (in tonnes), of each iceberg using the correlation of Robe and Farmer (1975): $M=3\,L\,W\,h$. We also used the maximum waterline length as the iceberg's characteristic length in later analyses.

Table 1 summarizes the iceberg and sea-state information obtained for each package deployment. Note that we encountered two main instrumentation difficulties during the 1985 field program. During four package deployments, the gyro experienced excessive vibration later attributed to contact-brush wear. This problem rendered the motion data unusable because we could not use the resulting pitch and roll data to remove gravitational components from the measured accelerations. The second problem was less severe: an intermittent short in the x-accelerometer circuit rendered data from

TABLE 1

Summary of iceberg and sea-state information for each motion-package deployment

Iceberg I.D.	Date (mm/dd/yy)	Characteristic length, L_c (m)	Mass (tonnes)	Significant wave height H_s (m)	Peak period T_p (s)	Wave spectrum	Motion data quality
1	08/02/85	13	590	0.69	6.6	no	good
2	08/05/85	22	4,400	0.91	9.5	yes	good
3	08/06/85	12	980	0.70	8.0	yes	A_x bad
4	08/06/85	26	7,900	0.64	8.3	yes	A_x bad
5	08/08/85	52	50,000	1.16	5.9	yes	data unusable
6	08/08/85	45	45,000	1.32	5.1	yes	good
7	08/10/85	140	1,000,000	0.92	7.3	no	good
8	08/11/85	70	120,000	0.71	6.8	no	data unusable
9	08/16/85	35	19,000	2.32	10.3	yes	good
10	08/18/85	110	730,000	2.03	10.0	yes	A_x bad
11	08/18/85	8.0	72	1.91	8.3	yes	data unusable
12	08/20/85	24	3,900	1.62	9.0	yes	A_x bad
13	08/21/85	53	54,000	1.51	10.3	yes	data unusable
14	08/21/85	13	780	1.23	8.3	yes	A_x bad
15	08/22/85	130	750,000	0.99	8.0	yes	good
16	04/27/86	3.3	14	0.6	2.8	no	good
17	04/29/86	6.8	27	1.8	4.9	no	good
18	03/19/87	8.0	120	1.7	5.9	no	good
19	03/19/87	8.0	120	1.7	5.6	no	good
20	03/28/87	3.5	10	2.2	5.3	no	good
21	03/31/87	14	420	1.6	10.4	no	good
22	04/17/87	10	80	2.0	5.8	no	good
23	04/20/87	5.0	30	2.2	4.8	no	good

that sensor unusable for five further deployments. However, we later developed a method to estimate significant surge and heave velocities using data from the working accelerometers. Thus, of the fifteen package deployments conducted in 1985, we obtained usable wave-induced motion data for eleven icebergs. These icebergs ranged in size from about 600–1,000,000 tonnes. They were floating in water depths of 60–300 m and experienced seas of 0.6–2.3 m significant wave height.

Grand Banks deployments

During March–April, 1986 and 1987, we deployed motion-monitoring packages on Grand Banks icebergs from an offshore supply vessel operated by Husky/Bow Valley (HBV) East Coast Project. The vessel possessed a water cannon which HBV used to deflect bergy bits and growlers away from its drilling platform. This arrangement put us near much smaller icebergs than we found in the Labrador Sea, and we obtained a total of eight package deployments.

To obtain sea-state information, we had originally expected to use data from a wave buoy moored at the HBV drilling platform. However, the vessel's iceberg management duties kept it well upstream of the platform, and all package deployments occurred more than 100 km away from the buoy. Therefore, we had to rely on sea-state estimates made by trained observers on board. We computed the observed wave height as the square root of the sum of the squares of their separate wind-wave and swell wave-height estimates. Jardine (1979) showed that this visual estimate tracks measured significant wave height.

We again used photographs taken from the vessel to document the size and shape of each iceberg studied. We encountered no instrumentation difficulties during the 1986/87 field programs and thus obtained eight usable data sets. Table 1 also summarizes the iceberg and sea-state information obtained during these Grand Banks deployments. The icebergs ranged in size from 10 to 420 tonnes and experienced seas of 0.6–2.2 m significant wave height. Figure 2 shows the motion-monitoring

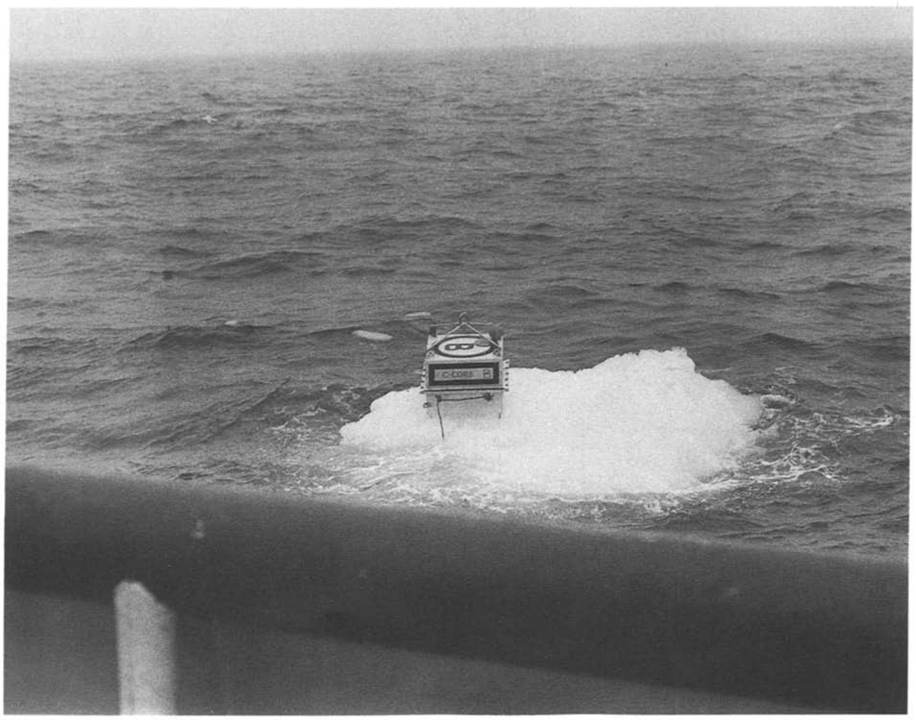

Fig. 2. Motion-monitoring package on iceberg 16, a 14-tonne growler in a 0.6-m significant-wave-height sea.

package on iceberg 16, a 14 tonne growler in a 0.6-m significant wave height sea.

Data reduction

Processing steps

Figure 3 shows a flow chart of the motion-data processing steps. We may identify three overall functions: primary processing, secondary processing, and data products.

Primary processing consisted of digitizing the original analog tape, demultiplexing, then converting the voltage signals to physical units for each sensor in the moving package reference frame. Because the digitizer operated at 1000 Hz, we averaged the digital voltages to achieve 12 Hz time series with improved signal/noise (about 60 dB). Frequency analysis of these signals showed only noise above 0.5 Hz. We therefore decimated (i.e., reduced) the data by a factor of 8 (to yield 1.5 Hz times series) then low-pass filtered from −0.1 dB at 0.5 Hz to −40 dB at 0.75 Hz.

Secondary processing consisted of transforming the motion data from the moving, package reference frame to a space-fixed, horizontal frame with axes pointing north, west and vertical. This transformation involved calculating, at each time step, the three modified Euler angles which uniquely define the package orientation with respect to the fixed frame. The gyro readings provided two of these angles directly, pitch and roll. The algorithm derived the remaining angle, yaw, from the compass reading.

We completed secondary processing by translating the fixed-frame accelerations from the package location to our estimate of the center-of-gravity (C.G.) of the iceberg. This is a straight-forward translation based on the following equation:

$$\mathbf{A}_{cg} = \mathbf{A}_p + \omega \times \omega \times \mathbf{R}_{cg} + \dot{\omega} \times \mathbf{R}_{cg} \quad (1)$$

where $\mathbf{A}_{cg}$ is the vector acceleration of the C.G., $\mathbf{A}_p$

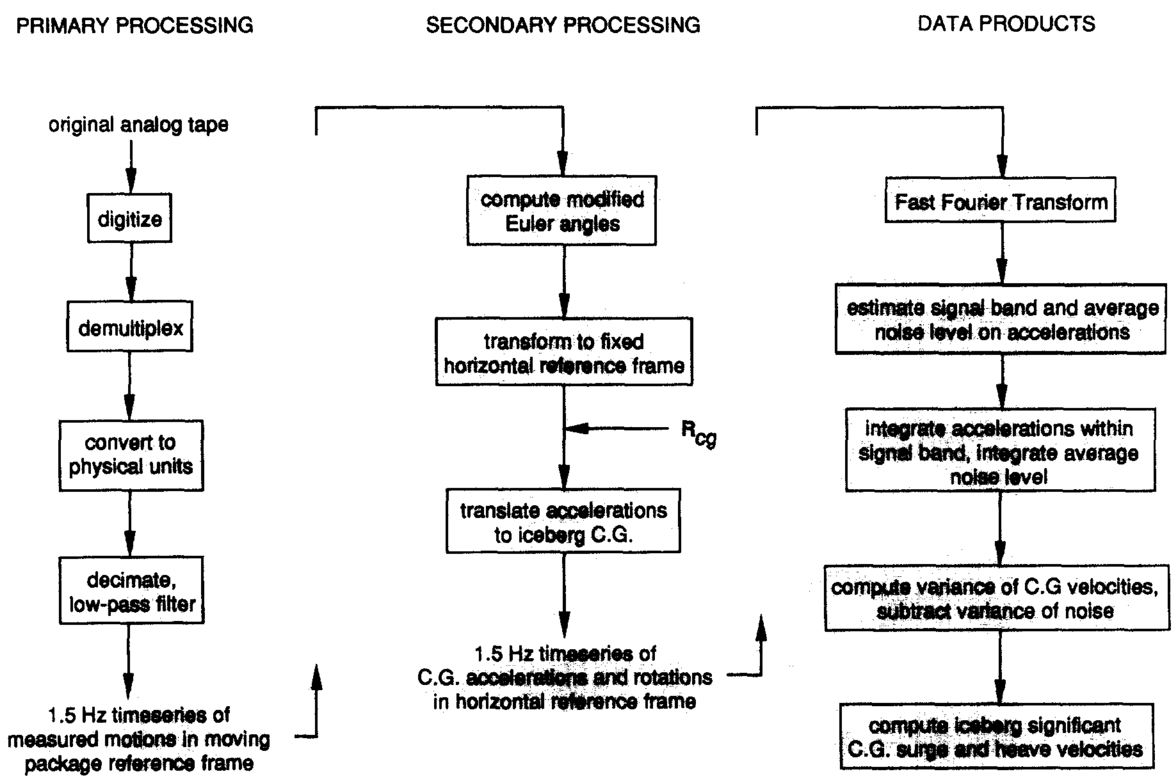

Fig. 3. Motion data processing steps.

is the vector acceleration of the package, ω is the angular rotation vector, and $\mathbf{R}_{cg}$ is the position vector from the package to the C.G.

To estimate $\mathbf{R}_{cg}$, we used photographs taken of the iceberg's above-water portion. Because each iceberg was stable at the time, the horizontal location of the C.G. coincided with that of the above-water portion. To estimate the vertical position of the C.G., we assumed an average iceberg C.G.-depth/height ratio of 1. For a perfectly tabular iceberg, with a draft/height ratio of 7.2, the C.G.-depth/height would be 3.6. However, field data show that average iceberg draft/height ratios fall in the range 2–4 (Robe, 1975; Hotzel and Miller, 1983) suggesting the use of substantially smaller C.G.-depth/height ratios than 3.6. Nevertheless, because these $\mathbf{R}_{cg}$ estimates were necessarily crude, we also conducted a study of the sensitivity of the C.G. velocities to variations in $\mathbf{R}_{cg}$.

Having obtained the acceleration of each iceberg's C.G., we then computed data products. For each deployment, we examined the frequency content of the accelerations using Fast Fourier Transforms. These spectra clearly showed wave-induced motion signals on top of essentially flat system noise. We integrated acceleration spectra to velocity spectra only within the identified signal bands, to avoid integrating low-frequency noise. Also, because noise is uncorrelated with signal, we subtracted the variance of the noise from the total variance to yield the variance of the motion signal. In this way, we removed system noise from iceberg significant velocity estimates:

$$V_s = 2(m_0 - n_0)^{1/2} \tag{2}$$

Where m_0 is the total velocity variance (zero-th moment of the velocity spectrum) and n_0 is the variance of the noise (on the velocity spectrum). Note that the data processing yields iceberg C.G. heave (vertical) velocity directly; iceberg C.G. surge ve-

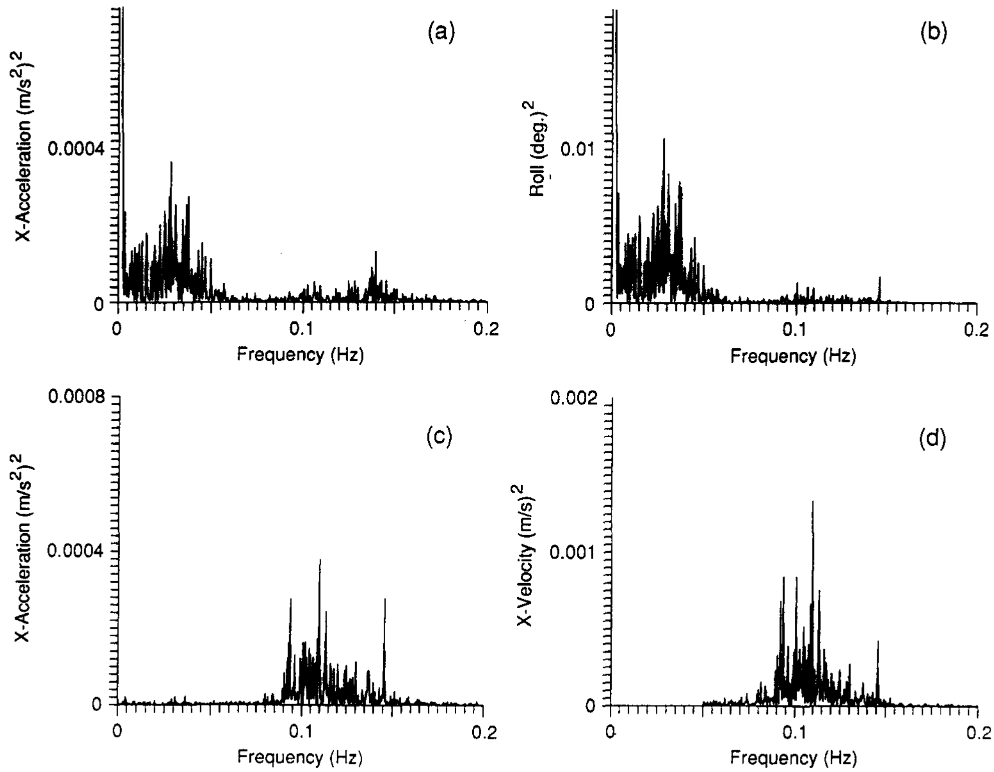

Fig. 4. Motion energy spectra for iceberg 9: (a) x-accelerometer in moving package frame, (b) gyro roll reading, (c) x-axis acceleration in horizontal reference frame, (d) x-axis velocity transformed to iceberg C.G. Note how transformation to a horizontal reference frame (c) removes low-frequency gravitational components in A_x (a) due to roll.

locity is the square root of the sum of the squares of the two horizontal C.G. velocity components.

Figure 4 shows Fourier spectra for iceberg 9, a 19,000-tonne bergy bit in 2.32 m seas. Notice how transformation to a horizontal reference frame removes gravitational acceleration components due to iceberg roll. The resulting horizontal-frame x-acceleration (Fig. 4c) shows wave-induced motion signals from 0.08 Hz to about 0.2 Hz. it also shows the characteristically flat system noise spectrum.

Error analysis

The principal data products of interest are iceberg significant surge and heave C.G. velocities, U_s and V_s, respectively. We may compare normalized forms of these, $U_s/(\pi H_s/T_p)$ and $V_s/(\pi H_s/T_p)$, against predictions based on wave-tank data (Lever et al., 1988b) for the same normalized peak wavelength, λ_p/L_c, where H_s is significant wave height, T_p is peak wave period, L_c is iceberg characteristic length (equal to maximum waterline length), and peak wavelength is given by:

$$\lambda_p = g\,T_p^2/2\,\pi \qquad (3)$$

This section discusses the uncertainty associated with each measured parameter and how these combine to influence the normalized significant velocities.

For the 1985 field season, we obtained sea-state data from a calibrated wave buoy moored near the study areas. We therefore expect about $\pm 5\%$ uncertainties in H_s and T_p derived from these data.

For the 1986 and 1987 field seasons, we obtained wave-height estimates from trained observers on the vessel. Based on the work of Jardine (1979), we expect observed wave height to equal H_s within about $\pm 40\%$. To obtain T_p for these deployments, we used the peak frequency in the measured velocity spectra. Because the icebergs studied in 1986/87 were quite small, we assumed that the peak period of the measured motion equalled T_p within an uncertainty of about $\pm 10\%$.

Photographs taken during package deployments provided the means to estimate L_c for each iceberg. This method leads to about $\pm 10\%$ uncertainty in L_c.

In addition, we used photographs to estimate $\mathbf{R}_{cg}$ for each iceberg. Although the uncertainty in $\mathbf{R}_{cg}$ might be as much as $\pm 50\%$, significant C.G. velocities are not very sensitive to this uncertainty. For the 1985 icebergs, $\pm 50\%$ variation in $\mathbf{R}_{cg}$ caused about $\pm 19\%$ variation in significant C.G. velocities; for the 1986/87 icebergs, the resulting variation was only $\pm 5\%$. Equation 1 reveals the reason for this insensitivity: rotational motions of small icebergs are much less significant than linear motions. Lever et al. (1989) observed a similar effect in their wave-tank study. When combined with uncertainty in the motion measurements themselves, we expect average uncertainties in significant C.G. velocities of $\pm 20\%$ for 1985 icebergs, and $\pm 7\%$ for 1986/87 icebergs.

The afore-mentioned uncertainties apply to most icebergs studied. However, we treated several 1985 deployments as special cases:

(a) For icebergs 6 and 15, the measured motions were sufficiently small that C.G. translation introduced excessive noise. For these two cases, therefore, we computed significant velocities only for the motion package location, then applied uncertainties of $\pm 20\%$ as if these were C.G. velocities.

(b) For iceberg 7, the measured motions were below the system noise level, implying negligible motion. This is a valid result, and we assigned significant surge and heave velocities of 1.0 ± 0.5 cm/s to this iceberg (i.e., just below system noise in the period band 5–15 s).

(c) For icebergs 3, 4, 10, 12 and 14, the x-accelerometer data (A_x) were unusable. To determine if we could nevertheless estimate U_s and V_s for these five cases, we examined the remaining complete data sets (1985–1987). We found that loss of A_x had a negligible effect on significant heave velocity. However, the surge-velocity variance dropped by a factor of 2, on average, without A_x. This implies that surge energy was nearly equally distributed along the x- and y-axes. Thus, for the five deployments with unusable A_x, we left the computed significant heave velocities unaltered, and we multiplied the computed significant surge velocities by $\sqrt{2}$. Study of the complete data sets suggested this latter operation increased the uncertainty in U_s by about 12%.

Using these estimates of uncertainty in the measured parameters, we may estimate uncertainty in the normalized significant velocities and peak wave lengths. Note that we may round the final uncertainty values to one significant figure, to reflect the precision of the contributing estimates. Thus, for the 1985 deployments, uncertainty in the normalized significant velocities is about ±20%, primarily reflecting the uncertainty associated with C.G. translation; the exception is iceberg 7, where ±50% uncertainty applies due to its small motion. For the 1986/87 deployments, the normalized significant velocities contain uncertainty of about ±40%, dominated by the large uncertainty associated with visual wave-height estimates. Similarly, the uncertainty in λ_p/L_c is about ±10% for the 1985 deployments and ±20% for the 1986/87 deployments; the difference reflects the larger uncertainty in T_p for the later deployments.

Discussion of results

Table 2 presents the significant surge and heave C.G. velocities for each iceberg with valid motion data. Also shown are the corresponding normalized peak wavelengths and significant velocities together with their uncertainties. We may compare these field results to predictions based on wave-tank data.

Lever et al. (1988a,b) measured response amplitude operators (RAO's) for four geometrically regular, model icebergs (cubical, cylindrical, trapezoidal, spherical). They then combined these RAO's with JONSWAP wave spectra to yield significant-velocity predictions for each shape. These curves of normalized significant velocity versus normalized peak wavelength form a basis for comparison between laboratory and field data.

TABLE 2

Iceberg significant velocities

Iceberg I.D.	Significant velocities		λ_p/L_c	Normalized significant velocities	
	Surge, U_s (cm/s)	Heave, V_s (cm/s)		$U_s/(\pi H_s/T_p)$	$V_s/(\pi H_s/T_p)$
1985			±10%	±20%	±20%
1	11	27	5.2	0.33	0.82
2	27	33	6.4	0.90	1.1
3	22	22	8.3	0.81	0.81
4	11	21	4.1	0.46	0.88
6	5.1	7.1	0.90	0.06	0.09
7	1	1	0.59	0.03	0.03
9	39	19	4.7	0.55	0.27
10	151	23	1.4	2.4	0.36
12	130	78	5.3	2.3	1.4
14	74	45	8.3	1.6	0.96
15	4.8	2.2	0.77	0.12	0.06
1986/87			±20%	±40%	±40%
16	52	64	3.7	0.78	0.96
17	77	81	5.5	0.67	0.70
18	92	114	6.8	1.0	1.3
19	92	119	6.1	1.0	1.3
20	110	119	12.5	0.85	0.92
21	78	94	12.1	1.6	2.0
22	46	46	5.2	0.42	0.42
23	111	113	7.2	0.77	0.78

Note that all velocities are for iceberg C.G. with the following exceptions: #7–motion signals below system noise level, velocities of 1 cm/s assigned (uncertainty ±50%); #6, 15–low signal/noise prevented translation to C.G., velocities are for package location.

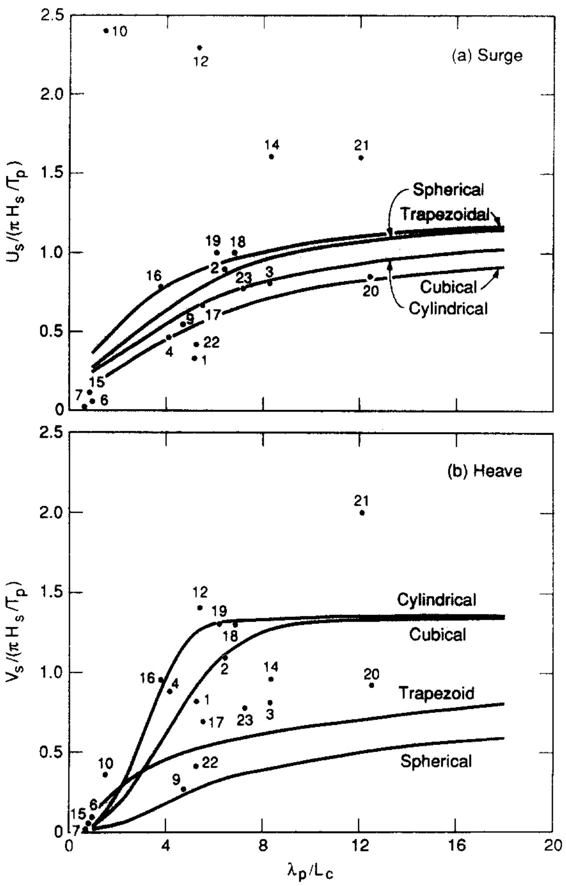

Fig. 5. Measured C.G. velocities compared with wave-tank based results for four regular shapes (Lever et al., 1988b).

Figure 5 presents a comparison between the field data and the laboratory-based predictions of Lever et al. (1988b). For most icebergs studied, the measured significant velocities fall within the range of the velocities predicted for the four regular shapes. That is, cubical, cylindrical, trapezoidal and spherical models reasonably represent the range of surge and heave velocities exhibited by irregularly shaped, full-scale icebergs.

As might be expected, several icebergs displayed motion well outside the range of the laboratory-based predictions. The most significant deviations exist for the surge velocities of icebergs 10, 12, and 14. Note that these were three of the five icebergs with unusable x-accelerometer data. Also, their surge velocities displayed above-average $\mathbf{R}_{cg}$ sensitivity. However, the significant heave velocities measured for these icebergs show much better agreement with prediction. This suggest that doubling the surge-velocity variance to compensate for loss of A_x yields poor approximations for these icebergs. The results for icebergs 3 and 4 (the other two cases of unusable A_x) agree much better with the predicted curves.

Only one Grand Banks iceberg showed substantial deviation from prediction. For iceberg 21, both the surge and heave significant velocities are much higher than expected. Interestingly, this is the only case where the swell-wave component dominated the visual sea-state estimate. The period of this component may well have coincided with the natural roll period of the iceberg, leading to resonance. Because the roll center need not be the C.G., such resonance would produce higher C.G. velocities than predicted for that significant wave height.

We also examined whether using measured wave-energy spectra significantly altered predicted velocities for the 1985 icebergs. Basically, we repeated the procedure of Lever et al. (1988b) using both the measured spectrum and a JONSWAP spectrum for values of H_s, T_p, and L_c obtained in the field. We then computed the mean and sample standard deviation of the normalized significant velocities predicted for the four regular iceberg shapes. Table 3 compares these predicted values and indicates whether agreement with the measured iceberg velocities improves by using the measured spectra. On average, measured wave spectra produced the same level of agreement with measured velocities as did JONSWAP spectra.

We may now address the key issue of the study: How well do velocity statistics derived for regular shapes reflect those of randomly shaped, full-scale icebergs? As with the sea-surface elevation itself, we may assume that iceberg open-water instantaneous surge and heave velocities possess Gaussian probability distributions. Because these velocities have zero mean, each distribution is a function only of the velocity variance, or equivalently, the significant velocity. Lever et al. (1989) derived a method to approximate iceberg/structure impact-velocity statistics from these Gaussian distributions. This is a useful simplification: with only knowledge of iceberg open-water significant surge and heave velocities, we may approximate the statistics of iceberg/structure impacts. However, U_s and V_s for a given

TABLE 3

Normalized significant C.G. velocities for the four regular iceberg shapes tested by Lever et al. (1988a) computed using both measured wave spectra and JONSWAP wave spectra

Iceberg I.D.	Normalized velocities using measured wave spectrum				Normalized velocities using JONSWAP wave spectrum				Change in agreement with measured velocities by using measured wave spectrum	
	Surge		Heave		Surge		Heave		Surge	Heave
	average	std.dev.	average	std.dev.	average	std.dev.	average	std.dev.		
2	0.67	0.13	0.61	0.31	0.78	0.14	0.81	0.45	worse	worse
3	0.77	0.15	0.67	0.31	0.87	0.14	0.87	0.46	better	worse
4	0.55	0.12	0.47	0.25	0.60	0.14	0.59	0.36	better	worse
6	0.20	0.06	0.07	0.04	0.17	0.05	0.02	0.03	worse	better
9	0.62	0.17	0.67	0.45	0.68	0.15	0.74	0.52	better	better
10	0.26	0.07	0.08	0.05	0.27	0.08	0.07	0.05	no change*	no change
12	0.70	0.13	0.75	0.45	0.69	0.14	0.72	0.43	no change	no change
14	0.83	0.13	0.82	0.40	0.87	0.13	0.89	0.46	no change	worse
15	0.16	0.05	0.04	0.02	0.16	0.05	0.02	0.02	no change	better

* "No change" in agreement indicates the two wave spectra yield results within 5% of each other.

TABLE 4

Mean and sample standard deviation of normalized significant C.G. velocities of the four regular iceberg shapes studied by Lever et al. (1988a,b)

λ_p/L_c	Normalized surge velocities				Normalized heave velocities			
	mean	std.dev.	low	high	mean	std.dev.	low	high
1.0	0.27	0.07	0.15	0.42	0.05	0.05	0.00	0.19
2.0	0.39	0.11	0.20	0.64	0.18	0.10	0.04	0.42
3.0	0.51	0.14	0.27	0.82	0.38	0.20	0.09	0.86
4.0	0.61	0.14	0.37	0.92	0.57	0.34	0.11	1.41
5.0	0.69	0.14	0.44	0.99	0.72	0.43	0.14	1.78
6.0	0.77	0.14	0.52	1.07	0.81	0.45	0.18	1.90
7.0	0.82	0.13	0.59	1.10	0.86	0.47	0.20	1.99
8.0	0.87	0.13	0.63	1.14	0.90	0.47	0.23	2.02
9.0	0.90	0.13	0.66	1.17	0.92	0.47	0.24	2.04
10.0	0.93	0.13	0.69	1.20	0.94	0.45	0.28	2.01
11.0	0.96	0.13	0.72	1.23	0.96	0.45	0.29	2.02
12.0	0.98	0.13	0.74	1.25	0.97	0.44	0.31	2.00
13.0	1.00	0.13	0.76	1.27	0.98	0.43	0.33	1.98
14.0	1.02	0.12	0.80	1.27	0.99	0.42	0.35	1.97
15.0	1.03	0.13	0.79	1.30	1.00	0.41	0.37	1.96
16.0	1.04	0.12	0.82	1.29	1.01	0.40	0.39	1.93
17.0	1.05	0.12	0.83	1.30	1.02	0.39	0.41	1.92
18.0	1.06	0.12	0.84	1.31	1.03	0.38	0.43	1.90

Low and high refer to the interval limits containing 95% of the cumulative probability assuming that a gamma distribution applies.

iceberg size and sea state depend on iceberg shape, another random variable. Therefore, we must describe variations in $U_s(H_s,T_p,L_c)$ and $V_s(H_s,T_p,L_c)$ in terms of appropriate probability distributions.

The response curves shown in Fig. 5 for the four regular iceberg shapes provide a way to estimate these probability distributions. At each λ_p/L_c, we may compute the mean and sample standard deviation of the predicted normalized significant velocities. We may then use these values to specify the parameters in a suitable probability distribution. The gamma probability density meets our requirements for a two-parameter distribution with a positive range:

$$p(x)=\begin{cases}\dfrac{c^{b+1}}{\Gamma(b+1)}x^{b}e^{-cx} & x\geq 0\\ 0 & x<0\end{cases} \tag{4}$$

where $c=\bar{x}/\sigma^2$ and $b=(\bar{x}^2/\sigma^2)-1$ and where $\bar{x}$ and σ are the mean and standard deviation, respectively.

Table 4 shows means and sample standard deviations of normalized significant velocities for the four regular iceberg shapes investigated by Lever et al. (1988a,b). To demonstrate whether a gamma distribution based on these wave-tank results fits the full-scale data, we computed the 95% cumulative

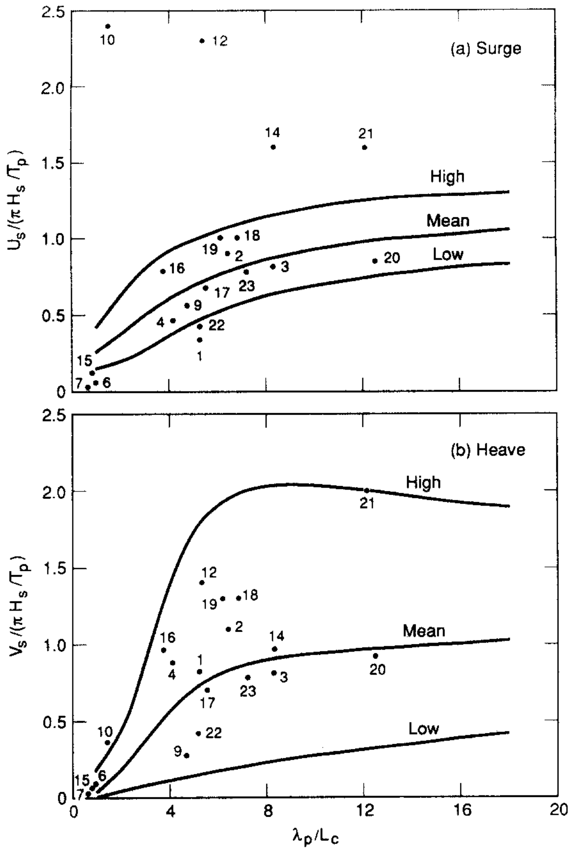

Fig. 6. Measured C.G. velocities compared with mean and 95% cumulative probability intervals derived from wave-tank results assuming that a gamma distribution applies. P (Low $\leq x \leq$ High) = 0.95.

probability interval at each λ_p/L_c; we would expect 2.5% of the velocities to fall outside this interval on each side. Figure 6 presents the measured full-scale velocities against the means and 95% intervals assuming gamma distributions.

Within the uncertainty of the field measurements, all measured heave velocities fall within the 95% interval. This interval is quite large for a given λ_p/L_c reflecting the pronounced influence of iceberg shape on heave motion. With uncertainty included, the only measured surge velocities substantially outside the 95% interval are those of icebergs 10, 12 and 14, the deployments identified earlier as having problems with loss of A_x data. Thus, within the accuracy of the field measurements, a gamma probability density fitted to wave-tank results describes the variation due to random shape of iceberg surge and heave significant velocities.

Conclusions

We met our original objective of obtaining field measurements of wave-induced iceberg motion as a function of iceberg size and sea state. A total of 23 motion-monitoring package deployments yielded 19 usable data sets, with a faulty gyro accounting for the data loss in the first year. Our experience has shown the package design and deployment/recovery operations to be successful. Indeed, C-CORE continues to use updated versions of these packages for unattended motion monitoring of icebergs, ice floes and sheet ice.

For comparison with laboratory measurements, we computed normalized full-scale significant velocities and normalized peak wavelengths. An uncertainty analysis revealed that inaccuracy in the measured motions ($\pm 5\%$) is relatively unimportant; depending on iceberg size, uncertainty in C.G. location can be much more significant ($\pm 20\%$ effect on 1985 C.G. velocities). In the absence of costly and time-consuming iceberg profiling, this source of uncertainty is unavoidable. However, its effect was much smaller for the small bergy bits and growlers studied in 1986/87 ($\pm 5\%$). Unfortunately, the lack of wave-buoy data overwhelmed the uncertainty for these later deployments ($\pm 40\%$ effect on normalized velocities). While this source of uncertainty can be avoided, the logistical difficulties of maintaining a wave buoy near a small ice mass in even moderate seas can be formidable. The use of two attending vessels would probably alleviate this problem, albeit at substantial added expense.

Within the measurement uncertainty, the present study confirms that wave-tank based velocities calculated for regularly shaped models do reflect the range of velocities observed for randomly shaped full-scale icebergs. Because of the strong influence of iceberg shape, we must treat surge and heave significant velocities as random quantities for a given iceberg size and sea state. The present work suggests that gamma probability densities fitted to wave-tank-based results are suitable for this purpose.

Acknowledgements

Of the numerous individuals who supported this study, several deserve special mention. Without Charlie Randell, at least two of the authors would not have survived construction of the motion packages. His good humor and tolerance served us well throughout the 1985 and 1986 field seasons. Denny Christian's logistical support, which at times included chasing runaway motion packages and wave buoys, was also vital to the success of the program. Additionally, the authors sincerely appreciated Dave Holland's seemingly endless struggle with the data-processing software and calibration studies.

We also gratefully acknowledge the Grand Banks deployment opportunities provided by Husky/Bow Valley East Coast Project, and the efforts of Greg Warbanski and Erik Banke in coordinating them. We further thank the Canadian Environmental Studies Research Funds for allowing us to merge logistical support with the DIGS experiment. In addition, Mike Lewis (Geological Survey of Canada) and Jack Clark (C-CORE) deserve our thanks for showing confidence in our approach and providing us organizational backing. Most importantly, the authors express their gratitude to the Natural Sciences and Engineering Research Council of Canada, and particularly the members of its Strategic Grants Program, for providing funding and moral support for such high-risk research.

References

Andersson, L., Lindberg, K. and Ygge, A., 1986. Structural safety of semis in sub-arctic waters. POLARTECH'86, Vol. 2: 540–555.

Fuglem, M.K., Duthinh, D., Lever, J.H. and Jordaan, I.J., 1991. Probabilistic determination of iceberg collision design loads for floating production vessels. Proc. IUTAM/IAHR Symp. Ice–Structure Interaction. in press.

Hodgson, G.J., Lever, J.H., Woodworth-Lynas, C.M.T. and Lewis, C.F.M. (Editors), 1988. The dynamics of iceberg grounding and scouring (DIGS) experiment and repetitive mapping of the eastern Canadian continental shelf. Environ. Studies Res. Funds Rep. 094, Vol. 1, 315 pp.

Holthe, K., 1989. A numerical model for predicting the response of concrete gravity platforms to iceberg impact. Proc. 10th Conf. Port and Ocean Engineering Under Arctic Conditions, Vol. I: 527–536.

Hotzel, I.S. and Miller, J.D., 1983. Icebergs: their physical dimensions and the presentation and application of measured data. Ann. Glaciol., 4: 116–123.

Isaacson, M. de St. Q., 1987. Ice mass motions near an offshore structure. J. Offshore Mech. Arc. Eng., 109(2): 206–210.

Jardine, T.P., 1979. The reliability of visually observed wave heights. Coastal Eng., 3(1): 33–38.

Lever, J.H., Klein, K. and Diemand, D., 1986. Design, development and deployment of instrument packages to monitor the motion of glacial ice masses at sea. Proc. 1st Int. Conf. Ice Technology, pp. 225–236.

Lever, J.H. and Sen, D., 1987. A method to upgrade iceberg velocity statistics to include wave-induced motion. J. Offshore Mech. Arc. Eng., 109(3): 278–286.

Lever, J.H., Attwood, D. and Sen, D., 1988a. Factors affecting the prediction of wave-induced iceberg motion. Cold Reg. Sci. Technol., 15(2): 177–190.

Lever, J.H., Sen, D. and Attwood, D., 1988b. The influence of shape on iceberg wave-induced velocity statistics. J. Offshore Mech. Arct. Eng., 112(3): 263–269.

Lever, J.H., Colbourne, B. and Mak, L., 1989. Model study of the wave-driven impact of bergy bits with a semi-submersible platform. J. Offshore Mech. Arct. Eng., 112(4): 313–322.

Pawlowski, J.S. and Wishahy, M.A., 1987. Time domain simulation of the drifting of small floating bodies in waves. Proc. 9th Conf. Port and Ocean Engineering Under Arctic Conditions, Vol. 1: 239–251.

Robe, R.Q., 1975. Height to draft ratios of icebergs. Proc. 3rd Conf. Port and Ocean Engineering Under Arctic Conditions, Vol. 1: 407–415.

Robe, R.Q. and Farmer, L.D., 1975. Physical properties of icebergs – total mass determination. Rep. Int. Ice Patrol Service in the North Atlantic Ocean, Season of 1975, U.S. Coast Guard Bull. 61, CG-188-30: 61–66.

Salvalaggio, M.A. and Rojansky, M., 1986. The importance of wave-driven icebergs impacting an offshore structure. Proc. 18th Offshore Technology Conf., Vol. 1: 29–38.